Published in Surf. Sci. 602, 2936 (2008).

Step Formation on Hydrogen-etched 6H-SiC{0001} Surfaces

S. Nie, C. D. Lee[§], and R.M. Feenstra[*]
Dept. Physics, Carnegie Mellon University, Pittsburgh, PA 15213, USA
Y. Ke, R.P. Devaty and W.J. Choyke
Dept. Physics and Astronomy, University of Pittsburgh, Pittsburgh, PA 15260, USA
C. K. Inoki and T. S. Kuan
Dept. Physics, University at Albany, SUNY, Albany, NY 12222, USA
Gong Gu
Sarnoff Corporation, CN5300, Princeton, NJ 08543, USA

The formation of step bunches and/or facets on hydrogen-etched 6H-SiC (0001) and $(000\bar{1})$ surfaces has been studied, using both nominally on-axis and intentionally miscut (*i.e.* vicinal) substrates. It is found that small miscuts on the (0001) surface produce full unit-cell high steps, while half unit-cell high steps are observed on the $(000\bar{1})$ surface. The observed step normal direction is found to be $<1\bar{1}00>$ for both surfaces. Hence, for intentionally miscut material, a miscut oriented towards this direction produces much better order in the step array compared to a miscut oriented towards a $<11\bar{2}0>$ direction. For (0001) vicinal surfaces that are miscut towards the $<1\bar{1}00>$ direction, the formation of surface ripples is observed for 3° miscut and the development of small facets (nanofacets) is found for higher miscut angles. Much less faceting is observed on miscut $(000\bar{1})$ surfaces. Additionally, the (0001) surface is found to have a much larger spatial anisotropy in step energies than the $(000\bar{1})$ surface.

I. Introduction

Vicinal surfaces, that is, surfaces cut on some small angle relative to a low-index face, have been widely used in semiconductor epitaxy as templates on which to grow well-ordered overlayers. For the case of SiC, a given polytype (*i.e.* a particular stacking arrangement) in the substrate can be preserved in homoepitaxial growth by the use of a stepped surface on the substrate [1]. For heteroepitaxy of GaN on SiC, vicinal surfaces of 6H-SiC(0001) have been found to be beneficial for reducing stacking fault density in the GaN [2]. Additionally, self-ordering of steps on semiconductors has attracted attention lately because of its potential use in patterning and fabrication of nanometer scale device structures [3].

There have been many reports concerning surface cleaning and smoothing of SiC to remove polishing damage on as-received substrates. High temperature etching in gaseous environments of H_2 [2, 4, 5, 6, 7, 8] or mixed H_2 and HCl [9, 10, 11] removes surface scratches effectively and generates atomically smooth surfaces. Step bunching and ordered step-terrace arrays are observed on etched surfaces and have been explained on the basis of differing etch rates for various types of steps [7, 8, 9] or by invoking a model of elastic interactions between steps [11].

[§] permanent address: Raytheon RF Components, Andover, MA 01810, USA
[*] author to contact: feenstra@cmu.edu

In this paper we report on the formation of step bunches and/or facets on H-etched SiC (0001) and $(000\bar{1})$ surfaces. We refer to the former surface as the *Si-face* and the latter as the *C-face*. We have studied both nominally on-axis and vicinal surfaces, with miscut angles of up to 12°. We find in general for very small miscut angle (<1º) that full unit-cell height steps occur on the Si-face, while for the C-face half unit-cell height steps are observed. Since the observed step normal direction is $\langle 1\bar{1}00\rangle$ (for both the Si-face and the C-face), it is found that a surface miscut in this direction shows much better order in the step array compared to a miscut in the $\langle 11\bar{2}0\rangle$ direction. For vicinal surfaces that are miscut towards the $\langle 1\bar{1}00\rangle$ direction, faceting is observed on Si-face surfaces whereas the C-face shows almost no faceting. The Si-face results extend over a much larger angular range and show significantly different spatial periods than in previous work [7,8], whereas for the H-etched miscut C-face there are no prior reports that we are aware of. The differences that we observe between the Si-face and C-face, full unit-cell steps and faceting in the former but not the latter, are interpreted in terms of differences in the etch rates of the various types of steps on the two faces.

II Experimental

SiC (0001) Si-face and $(000\bar{1})$ C-face surfaces were studied, using both 6H and 4H polytype substrates. Results from the two polytypes were similar, and only data from the former are reported here. The 6H substrates were n-type with resistivities in the range 0.03 – 3 ohm-cm. The surfaces were miscut away from the nominal (0001) or $(000\bar{1})$ planes by angles as large as 12°, with the direction of miscut being towards either the $\langle 1\bar{1}00\rangle$ or $\langle 11\bar{2}0\rangle$ directions. On-axis substrates as well as substrates miscut at 3.5° towards $\langle 11\bar{2}0\rangle$ were purchased from Cree Corp. Other substrates used were cut from boule material and mechanically polished with diamond paste with decreasing grit size down to 0.25 μm, and for these samples the miscut angle was checked with x-ray diffraction; these miscut angles have an accuracy of ±0.2°.

A homebuilt strip-heater employing a Ta strip is used for H-etching [12]. The 1 cm × 1 cm sample rests on a 0.001 inch thick Ta strip through which 70 A passes, heating the sample to high temperature. Hydrogen-etching is done in 1 atm of pre-purified (99.995%) hydrogen gas at a flow rate of 11 liters-per-minute for 100 seconds, with the sample held at a temperature in the range 1600 - 1650°C. The hydrogen flow over the SiC starts prior to the rise in temperature and ends after the wafer is cool. Cooling of the sample is done by switching off the power supply, producing a cooling rate of >100°C/s, although cooling rates of ≈10°C/s were also investigated and they produced no change in the results. Temperature is monitored by a disappearing filament pyrometer, with the sample viewed through a window in the etching chamber. Auger electron spectroscopy performed on the samples following the H-etching reveals a very small Ta peak, near the noise limit of the spectrum, implying a Ta surface coverage of about 0.03 monolayers.

After H-etching the substrates are cleaned in acetone, methanol, and deionized water, using an ultrasonic bath. Atomic force microscopy (AFM) is done using either a Park Scientific instrument in contact mode, or a Digital Instruments Nanoscope III in tapping mode. Transmission electron microscopy (TEM) was performed using a JEOL JEM-2010 transmission electron microscope operating at 200 kV.

III. Results

A. Nominally on-axis surfaces

For nominally on-axis substrates, H-etching produces uniformly distributed step-terrace arrays on both Si- and C-face surfaces, as shown in Fig. 1. The step arrays form because of the unintentional miscut of the surface (the *average* miscut values for the substrates of Figs. 1(a) and (b) are 0.28 and 0.18°, respectively, although these values differ from the *local* miscut of the observed step arrays of 0.41 and 0.11°, respectively, due to the formation of large-scale low-angle facets on such surfaces as previously described [5]). Step edges perpendicular to $<1\bar{1}00>$ directions are observed for both faces. Following other authors, we conclude that these step directions have the lowest surface energy among all directions in the (0001) basal plane, or in other words, the H-etching is slowest in these directions [7, 8, 9]. The observed step height from Fig. 1 is 1.5 nm (*i.e.* six bilayers) for the 6H-SiC Si-face while it is 0.75 nm (three bilayers) for the 6H-SiC C-face, that is, a full unit-cell height in the former case and a half unit-cell height for the latter. The reason for this difference in step height between the Si- and C-faces will be discussed in Section IV.

.

B. Vicinal surfaces miscut towards $<1\bar{1}00>$

On vicinal surfaces, the width of terraces and the morphology of steps depend on miscut direction and angle. We first consider miscut angles towards $<1\bar{1}00>$, *i.e.* the same direction as the normal direction for low-energy steps. For small miscuts of <1° the steps maintain their equidistant arrangement. However, at higher miscuts a new phenomenon occurs, as shown in Fig. 2 for 6H-SiC Si-face surfaces miscut at 1° and 3°. Individual steps are clearly resolved on both surfaces, Figs. 2(b) and (d), and they have full unit-cell height. However, an additional feature seen in both images is a rippling of the surface morphology. This rippling persists over the entire surface, and has an average period in Fig. 2(a) of about 2 μm and in Fig. 2(c) of about 500 nm. [The line scan in Fig. 2(c) shows only the long-range modulation in surface height, with the individual unit-cell high steps being too closely-spaced to be resolved, although they are clearly seen in Fig. 2(d).] These relatively long-wavelength oscillations are consistent with our prior study in which we found a period of about 300 nm on a surface miscut at 3.5° towards $<1\bar{1}00>$ (although individual atomic steps were not resolved in that work) [2]. In general, this rippling is indicative of step-step separations that are no longer constant, but have some small periodic variation over the surface. Steps are closer spaced at the ascendant part of a ripple than at the descendant part. It should be noted that this type of arrangement occurs *without* forming any specific high-index crystal planes (*i.e.* facets) on the surface. An additional feature evident in Fig. 2(b) is that *orientation* of the steps is not perfectly constant (*i.e.* the steps are slightly curved), an issue that we return to in Section V.

With an even higher miscut of 5° the periodic undulations on the surface become much smaller in spatial period, as illustrated in Fig. 2(e). Individual steps of full unit-cell height (1.5 nm) are clearly visible in this image (about 35 steps are apparent, with the step edges extending vertically across the image). These individual steps tend to group together producing undulations with period of < 100 nm. The undulation pattern is somewhat irregular on the surface, but nevertheless on the right-hand side of Fig. 2(e) one can clearly see groups of about 6 unit-cell high steps giving rise to an undulation period of about 80 nm. Following prior work we denote these features as *nanofacets* [8]. The line scan shown in the inset of Fig. 2(e) clearly shows small (0001) terraces separated by the nanofacets.

Nanofaceting of the Si-face persists at higher miscut angles. We show in Fig. 3(a) an AFM image of the Si-face with a 12° miscut, and Fig. 3(b) shows data for the C-face with the same miscut. In both cases a closely-spaced array of steps is visible on the images, with the apparent step separation being significantly less for the C-face than for the Si-face. We find an average separation between linear (approximately periodic) features seen in the images of 19 nm for the Si-face and 7 nm for the C-face. For comparison, given the 12° miscut of the surfaces, if the surface consists of unit-cell high steps (as occurs for the Si-face with low miscut angle) then we would expect a 7.0 nm step-step separation, or if the surface consists of half unit-cell high steps (as occurs for the C-face with low miscut angle) then we would expect a 3.5 nm separation. Thus, we conclude from the data of Fig. 3 that for the Si-face we appear to be resolving step bunches of typical height 2 – 3 unit cells, whereas for the C-face we are resolving steps of single unit-cell height.

Our conclusions based on the AFM data are supported, and clarified, by cross-sectional TEM of the same samples, as shown in Fig. 4. On the Si-face, Fig. 4(a), faceting of the surface is clearly observed, with the appearance of $(1\bar{1}0n)$ facets having n ≈ 12 and making an angle of ≈25° to the (0001) planes. A similar facet angle for the Si-face has been reported previously [8]. From the TEM data we find typically 4 – 5 unit cell heights separating the observed (0001) terraces, which is similar (slightly larger) than the value deduced from the AFM images. For the C-face, minimal faceting is observed; any apparent step bunches involve only single or perhaps double unit-cell height steps. We cannot distinguish on the TEM image of Fig. 4(b) any distinction between single or half unit-cell high steps, but in any case the image is consistent with the AFM data of Fig. 3(b) that suggests single unit-cell high steps for this highly miscut C-face surface with no evidence of nanofaceting.

C. Vicinal surfaces miscut towards $<11\bar{2}0>$

We now turn to surfaces miscut towards $<11\bar{2}0>$, a miscut direction that is commonly used in epitaxial growth [13]. Since this direction does *not* correspond to the low-energy step direction for our H-etched surfaces, we find in general much less order in the resulting step array than for the $<1\bar{1}00>$ miscut direction of the previous section.

Results for the Si-face are shown in Figs. 5(a) and (b). At 3.5° miscut we observe zigzag step edges with half unit-cell height (0.75 nm), as shown in Fig. 5(a). The *average* direction of each step has step normal towards the $<11\bar{2}0>$ miscut direction, but *locally* the step edges appear to have a zigzag shape alternating portions being locally perpendicular to $<1\bar{1}00>$ directions. We thus interpret the step edge morphology as having many kinks, in the manner described by Nakajima *et al.* in Fig. 6 of their work [8]. It should be noted that this morphology is dependent on the etching method and conditions. Other etching methods ($HCl+H_2$) have given straight step edges with $<11\bar{2}0>$ step normal, or "triangular depressions", depending on the etching temperature [10]. The occurrence in our study of the local $<1\bar{1}00>$ step morphology is further evidence that, for H-etching, the etching rate along $<1\bar{1}00>$ is slower than that along $<11\bar{2}0>$. At a higher miscut angle of 12°, no *average* step orientation is found, as shown in Fig. 5(b). The steps are seen to meander all over the surface. Saitoh *et al.* [14] have reported similar surface morphology of an epilayer on a 4H-SiC Si-face substrate with 18º miscut towards $<11\bar{2}0>$. The reason for this change in morphology as the miscut angle increases is not well understood at present, but it is perhaps not so surprising that for a surface with such a high kink density (*i.e.* as occurs for steps with *average* orientation of $<11\bar{2}0>$) a nonuniform distribution of step spacing results.

In contrast to the Si-face results, the C-face miscut at 3.5° toward $<11\bar{2}0>$ displays full unit-cell high steps with step normal of $<11\bar{2}0>$, as shown in Fig. 5(c). Thus, for the C-face, steps perpendicular to $<11\bar{2}0>$ are found to have comparable stability to those perpendicular to $<1\bar{1}00>$. This conclusion is further confirmed by observations over a range of miscut orientations as occurs for steps surrounding a screw-type dislocation, as discussed in the following section. For a 12° miscut on the C-face, Fig. 5(d), an average orientation more nearly towards $<11\bar{2}0>$ is found, a result that is also consistent with the discussion in the following section where we argue that the change in energy of different step orientations for this surface is much smaller than for the Si-face.

IV. Discussion

In the previous section, we have reported two major differences between the surface morphologies of stepped Si-face and C-face SiC{0001} surfaces: (i) for low miscut angles, single unit-cell high steps are observed on the Si-face whereas half unit-cell high steps are found on the C-face, and (ii) for high miscut angles, the Si-face shows faceting whereas the C-face does not. We discuss in this section the underlying mechanisms behind these phenomena. Prior work has focused primarily on the Si-face, and our experimental results are generally in good accordance with those works [4-11]. The C-face has been less well explored, with our observations providing significant new insight into that surface.

Concerning the difference in steps heights between the Si-face and C-face, this arises from anisotropy in surface energies between the various possible terminating planes of the surface, as has been discussed for the Si-face by previous authors [7,8,15]. For 6H stacking, 3 of the 6 bilayers will contain double bonds for an abrupt termination at a step edge perpendicular to $<1\bar{1}00>$, and the other 3 bilayers will contain single bonds. (Of course, surface reconstruction can modify the structure at steps, but the *inequivalence* between the two groups of planes will remain). In general the surface energies of the various possible bilayers may differ, and indeed bulk energetics tends to favor termination on the particular bilayers containing hexagonal sites [15], *i.e.* one particular plane within each group of 3 bilayers; following Ref. [7] we denote these stable planes as S_N and S_D for the single and double bonds at the step edge, respectively. Step bunching during etching is visualized as a reverse process of step-flow growth. Thus, given the relative stability of S_N and S_D, we expect them to etch slower than the other planes. If these two planes etch with similar speed then half unit-cell high steps on the surface would be formed. Alternatively, if they etch with different speed (due to their inequivalence) then full unit-cell high steps would form. This latter situation is what we believe occurs on the Si-face, and the former situation on the C-face.

This interpretation of the differing step heights on Si-face and C-face surfaces forming as a result of differing step anisotropy in the two cases is further supported by observations of the morphology of steps around a screw dislocation, as shown in Fig. 6. For the C-face surface shown there, half unit-cell high steps are observed with circular shapes. As one goes around a step edge, the termination of the steps changes between S_N and S_D (for each 60° rotation around the center of the circle), and hence the observation of the circularly-shaped step edges demonstrates the near equivalence in the step energy for S_N and S_D on the C-face. In contrast, around a screw dislocation on the Si-face one observed full unit-cell high steps with a distinctly hexagonal arrangement of the step edges, as previously reported (Fig. 2 of Ref. [5], or Fig. 7 of Ref. [8]). In that case, there is a strong preference for one particular step edge.

Now we turn to the changes in the apparent rippling and facet formation observed on the Si-face but not the C-face, as the miscut angle of the wafer increases. For low miscut angles, Fig. 1(a), step trains with equidistant steps are formed. This situation is not surprising, since the large step height and stiffness of SiC result in a strong elastic repulsion force between steps [16]. (Entropic repulsion may also act to keep the steps apart [17], although the fact that we observe very straight steps indicates that our temperatures are not high enough for this effect to be relevant.) For larger miscut angles, we observe the formation of ripples in the Si-face surface morphology, Figs. 2(a) and (c), and finally complete nanofacet formation, Fig. 2(e). Wulfhekel *et al.* have noted the need for an attractive step-step interaction term to produce this behavior [7], *i.e.* in addition to the repulsive term due to strain interactions discussed above, although no specific mechanism was indicated. We suggest that a likely mechanism is an inverse Ehrlich-Schwoebel barrier (as has been discussed for SiC and Si surfaces in contexts other than H-etching [15,16,18]), in which H atoms collected on terraces preferentially etch upward steps thus causing larger terraces to collect more H atoms and hence grow even larger. Actually, this mechanism is an extension of the one discussed above for the formation of the unit-cell high or half unit-cell high steps, in that we are now specifying that the etching preferentially occurs from the lower terrace. Some combination of the strain effects and the inverse Ehrlich-Schwoebel barrier would then produce the observed behavior. For example, elastic effects might tend to maintain equidistant steps, but the etching kinetics produce an instability in the step-step separation. Or alternatively, the step-step strain interaction could modify the inverse Ehrlich-Schwoebel barrier itself, changing the kinetics from preferential etching on downward steps to preferential etching on upward steps as the step-step separation decreases. More detailed analysis is needed to fully identify the precise mechanisms involved.

For the Si-face with miscut towards $<1\bar{1}00>$, the above type of mechanism could account for *both* the formation of the unit-cell high steps at low miscut angles and for the formation of the nanofacets at higher miscut angles. For the C-face, apparently the asymmetry in etching-rates between S_N and S_D steps is less, so that half unit-cell high steps occur for low miscut, and for the same reason the nanofaceting type of instability is also less at the higher miscut angles than for the Si-face.

In general our studies are in very good agreement with those of Nakajima *et al.,* who studied H-etching of the Si-face miscut in various directions [8]. One notable exception to this agreement occurs, however, in those authors' observation for $<1\bar{1}00>$ miscut angles of an onset of the nanofaceting, with lateral period of about 150 nm for angles in the range 0.5° – 2°. In our case we observed surface rippling with periods of about 2000 and 500 nm for miscut angles of 1° and 3°, respectively. For larger miscut of 5° we found nanofaceting with period of about 80 nm, and at 12° the period is further reduced to about 20 nm. Thus, although the rippling/nanofaceting we observe is qualitatively similar to that seen by Nakajima *et al.*, the dependence of the lateral period on miscut angle is quite different. Also comparing to the work of Wulfhekel *et al.* [7], they found a period of about 1000 nm at 5° miscut. We tentatively ascribe these discrepancies to possible variations in surface preparation.

We also comment on an additional prior work, namely the study of Si-face surfaces miscut towards $<11\bar{2}0>$ by Fujii *et al.* [11], with which we have several differences. First, their steps display single unit-cell height whereas we observe zigzag half unit-cell high steps edges (in agreement with Nakajima *et al.* [8]), but we assume that this difference is due to the different etching conditions used.[1] Second, we point out for clarity that the term "nanofacets" is used by Fujii *et al.* to refer to the arrangement of bilayers that make up a *single* unit-cell high step, whereas in the present work as well as in Ref. [8] this term is used to refer to *multiple* unit-cell high steps. In any case, we certainly agree with Fujii *et al.* concerning the arrangement of bilayer steps that make up a single unit-cell high step. Concerning the *mechanism* for the formation of the single unit-cell high steps, however, we argued above that they arise from the different etching rates of the various steps, whereas Fujii *et al.* argued that they arise from an instability based on elastic strain that affects the interactions between steps. In our opinion, the true mechanism cannot be definitely determined without a more quantitative comparison of experiment with theory (for both the differing etch-rate model as well as the elastic strain model), but nevertheless we favor the mechanism of different etch-rates since this model may also provide explanations for the observed multiple unit-cell high steps as well as for the differing results for single unit-cell high steps between the Si-face and C-face and between $<1\bar{1}00>$ and $<11\bar{2}0>$ miscut directions.

V. Conclusion

Step arrays on vicinal SiC (0001) and $(000\bar{1})$ formed by H-etching are studied by AFM. H-etching leads to full unit-cell high steps on Si-face surfaces, but gives half unit-cell high steps on C-face surfaces. These observations are consistent with an asymmetry in the surface energy (*i.e.* etch rate) of the two types of step terminations occurring on the different surfaces. Nanofacet formation is observed on the vicinal Si-face, and is attributed to preferential etching from the lower terrace which leads to an instability in the step-step separations. The nanofacet formation is much less pronounced on the C-face, apparently due to more symmetric etching probabilities from both upper and lower terraces in that case.

---

[1] The etching gas in Ref. [11] is stated as H_2, but judging from the relatively low etching temperatures we assume that a small amount of HCl is present, as in the previous work, Ref. [10], from the same group.

We have noted the possibility of other mechanisms for the faceting phenomenon, including the elastic strain mechanism discussed in Ref. [11]. One additional mechanism briefly mentioned in prior work [8] is the possibility of low-energy faceted surfaces, as occurs *e.g.* in the faceted Si(111) surface when comparing flat 7×7 reconstructed regions to vicinal nonreconstructed regions [17]. The difference in surface energy due to the reconstruction provides the possibility of the facet formation in that case [17]. For the present situation on SiC{0001} we do not know the surface termination at high temperature with certainty, but a difference in reconstruction of the terraces separating the unit-cell high steps on the faceted surface seems highly unlikely and hence a faceting mechanism analogous to that seen in miscut Si(111) is quite improbable.

A major motivation for the present study of the morphology of vicinal SiC surfaces was to understand, and hence control, the surface morphology of SiC{0001} surfaces so that they can be used as a template for further epitaxial growth, *e.g.* formation of quantum wires at step edges. Production of a regular array of steps on the surface is, in general, what is desired for such applications. We have found here that C-face surfaces are much less prone to step bunching and/or nanofacet formation, and hence the separation of steps on those surfaces is much more uniform than for the Si-face. In this sense the C-face is superior as a template for use *e.g.* in forming quantized one-dimensional systems.

An additional consideration for the production of uniform step-terrace arrays arises from the inherent error in the miscut angle due to limitations in the accuracy of sample mounting. For low miscut angles, near 0°, this uncertainty gives rise to the varying domains of steps with different $<1\bar{1}00>$ orientations [5]. This situation may be quite undesirable in circumstances where one wants a more uniform step orientation over the entire sample. As a solution to this problem, we have found that the error in the miscut angle can be much better accommodated when it occurs on an *intentionally* miscut sample. For example, we return to Fig. 2(b) which shows a Si-face surface miscut at 1° towards the $<1\bar{1}00>$ direction. The step direction there is seen to be *not* perfectly constant on the surface, due to error in the miscut. But this error is now accommodated by a slight curvature in the step edges rather than the formation of low-angle facets with steps directed along a different $<1\bar{1}00>$ orientation. In this way, we have achieved a quite well ordered step-terrace array, extending over the entire sample.

Acknowledgements

This work was supported the National Science Foundation, grant DMR-0503748. Discussions with Luxmi are gratefully acknowledged.

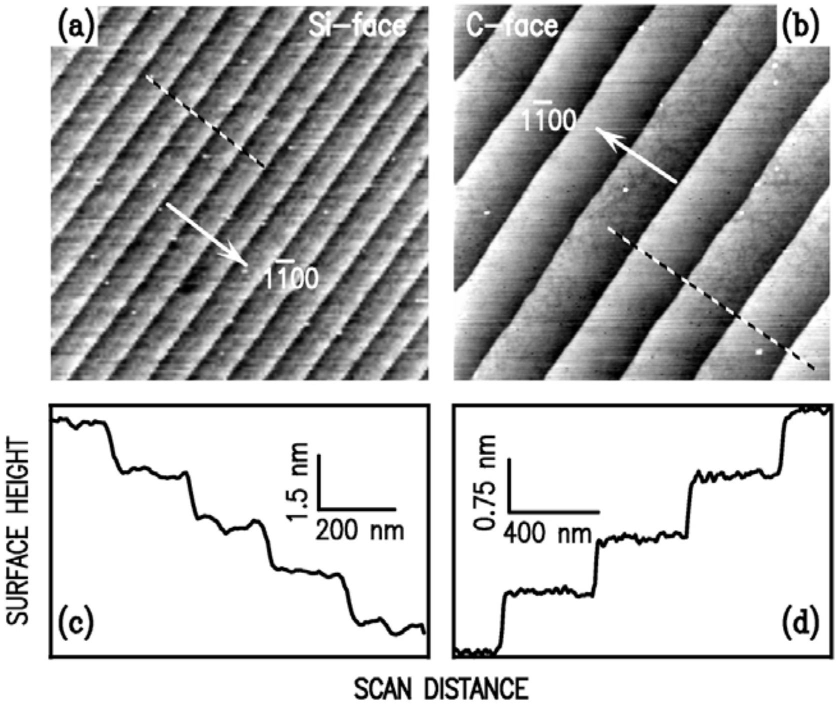

FIG 1. AFM images of nominally on-axis 6H-SiC surfaces: (a) Si-face and (b) C-face. Steps edges are normal to $<1\bar{1}00>$ directions. Dashed lines indicate the paths of the line scans displayed in (c) and (d), respectively. The images are displayed with grey scale ranges (height difference between white and black gray levels) of (a) 1.4 nm and (b) 0.9 nm. A linear background subtraction has been applied to the data of (c) and (d) compared to that of (a) and (b).

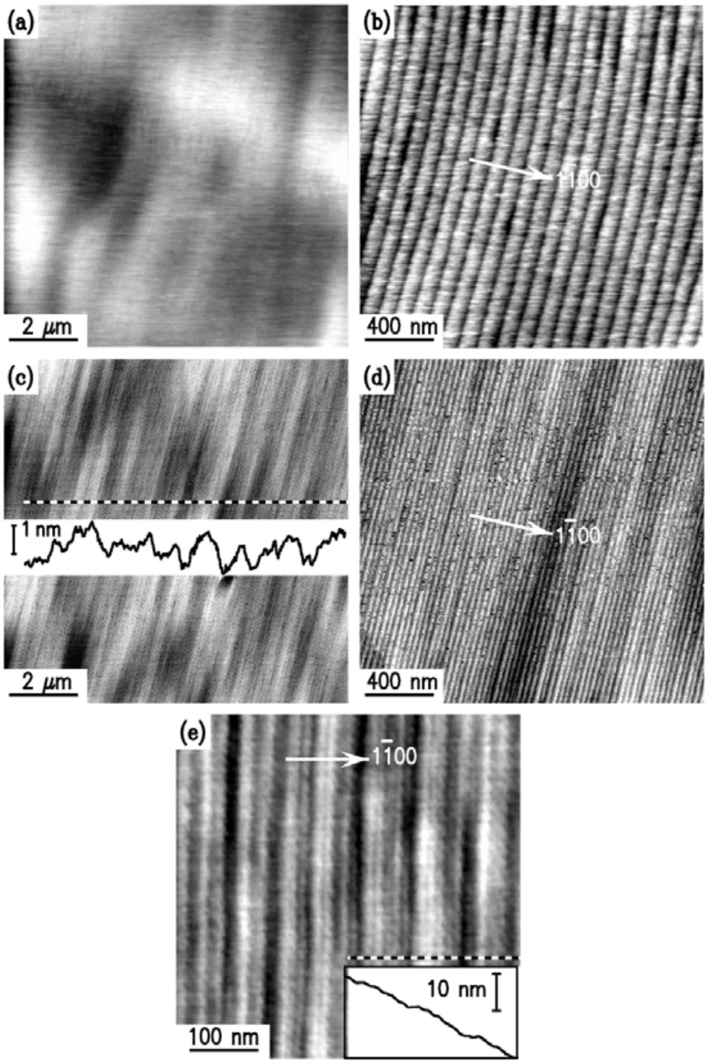

FIG 2. AFM images of 6H-SiC Si-face surfaces, miscut at various angles towards <1$\bar{1}$00>: (a) and (b) 1° miscut, (c) and (d) 3° miscut, (e) 5° miscut. The line cuts shown in the insets of (c) and (e) are taken along the dashed line in the images [a linear background subtraction has been applied to the line scan in (e) such that the (0001) terraces are horizontal]. Grey scale ranges are 3.2, 1.1, 2.7, 1.5, and 2.8 nm, for (a) – (e), respectively.

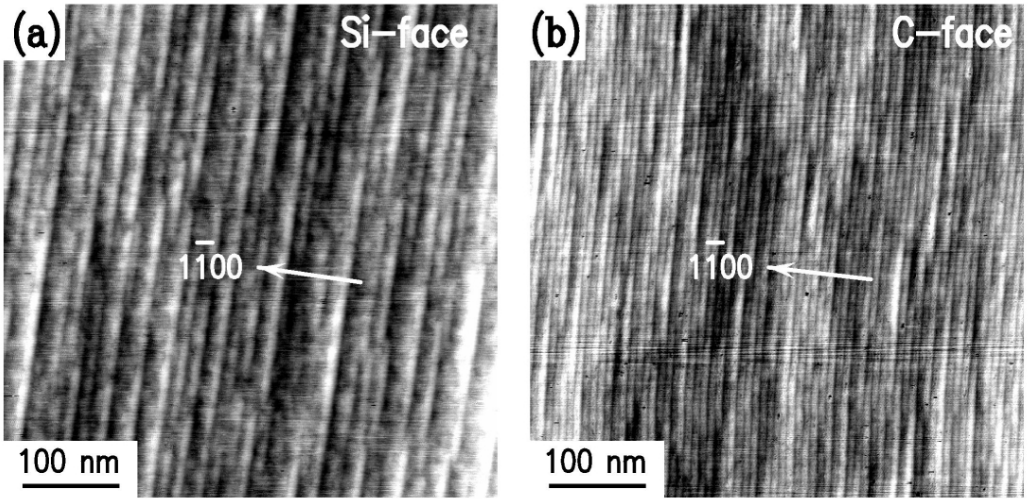

FIG 3. AFM image of H-etched 6H-SiC surfaces miscut at 12° off towards $<1\bar{1}00>$: (a) Si-face and (b) C-face. Grey scale range is 1.4 nm for both images.

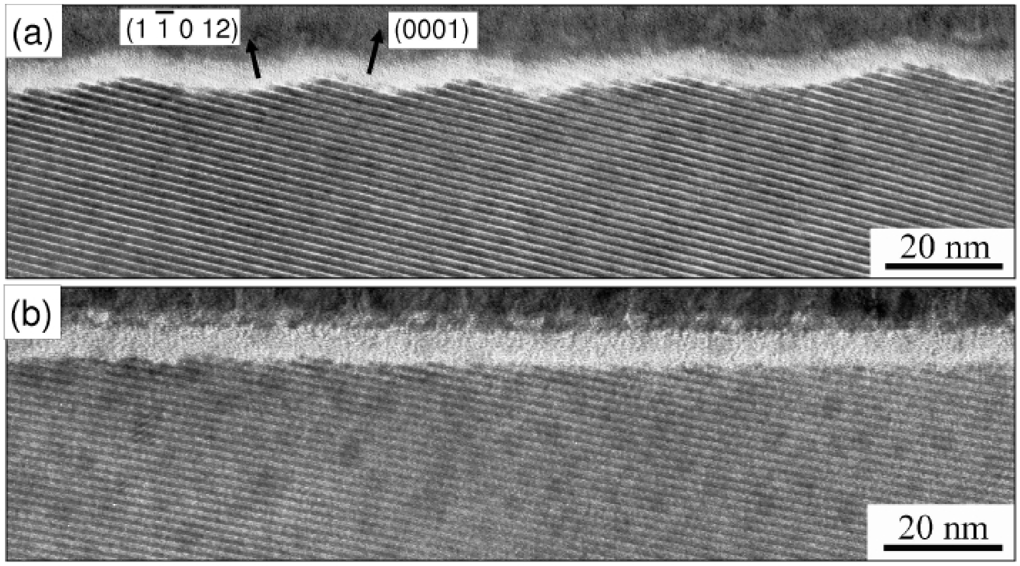

FIG 4. Cross-sectional TEM images obtained from the same samples pictured in Fig. 3, 6H-SiC miscut at 12° towards $<1\bar{1}00>$: (a) Si-face and (b) C-face. In the former case, facet orientations of (0001) and $(1\bar{1}0n)$ with n ≈ 12 are seen on the surface, whereas in the latter case only an average orientation 12° from $(000\bar{1})$ is observed. Both images are acquired with the electron-beam directed along $<11\bar{2}0>$.

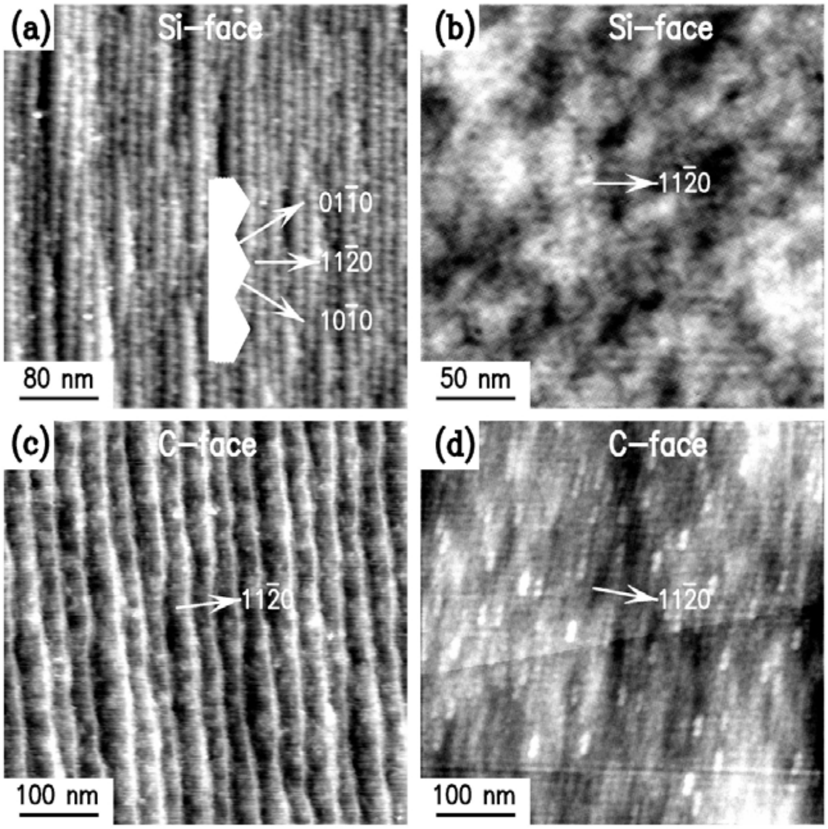

FIG 5. AFM image of 6H-SiC surfaces miscut at various angles towards $<11\bar{2}0>$: (a) Si-face with 3.5° miscut, (b) Si-face with 12° miscut, (c) C-face with 3.5° miscut, (d) C-face with 12° miscut. The white triangular schematic in (a) shows a step edge in expanded view, with step edge segments locally normal to $<1\bar{1}00>$ directions. Grayscale ranges are 0.8, 0.5, 1.3, and 0.7 nm for (a) – (d), respectively.

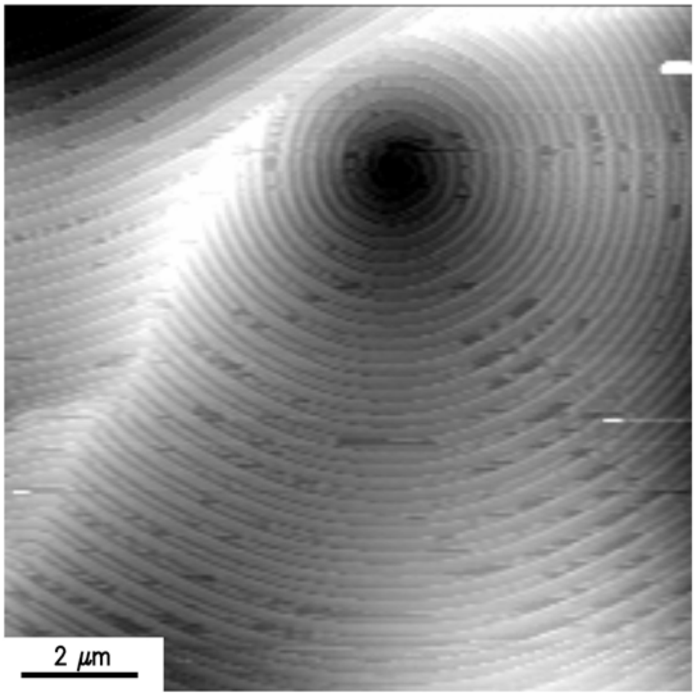

FIG 6. AFM image near a screw dislocation on a 6H-SiC C-face surface. Half-unit-cell height steps occur, with the step edges forming nearly circular shapes. Grayscale range is 8.0 nm.

References

---

[1] T. Kimoto, H. Nishino, W. S. Yoo, and H. Matsunami, J. Appl. Phys. **73**, 726 (1993).

[2] C. D. Lee, R. M. Feenstra, O. Shigiltchoff, R. P. Devaty , and W. J. Choyke, MRS Internet J. Nitride Semicond. Res. **7**, 2 (2002).

[3] M. Kawamura, N. Paul, V. Cherepanov, B. Voigtländer, Phys. Rev. Lett. **91**, 096102 (2003).

[4] F. Owman, C. Hallin, P. Mårtensson, E. Janzén, J. Cryst. Growth **167**, 391 (1996).

[5] V. Ramachandran, M. F. Brady, A. R. Smith, R. M. Feenstra, and D. W. Greve, J. Electron. Mater. **27**, 308 (1998).

[6] A. Kawasuso, K. Kojima, M. Yoshikawa, H.. Itoh, and K. Narumi, Appl. Phys. Lett. **76**, 1119 (2000).

[7] W. Wulfhekel, D. Sander, S. Nitsche, F. Dulot, A. Leycuras, and M. Hanbücken, Surf. Sci. **550**, 8 (2004).

[8] A. Nakajima, H. Yokoya, Y. Furukawa, and H. Yozenu, J. Appl. Phys. **97**, 104919 (2005).

[9] S. Nakamura, T. Kimoto, H. Matsunami, S. Tanaka, N. Teraguchi, and A. Suzuki., Appl. Phys. Lett. **76**, 3412 (2000).

[10] H. Nakagawa, S. Tanaka, and I. Suemune, Phys. Rev. Lett. **91**, 226107 (2003).

[11] M. Fujii and S. Tanaka, Phys. Rev. Lett. **99**, 016102 (2007).

[12] V. Ramachandran, Ph.D. thesis, Department of Physics, Carnegie Mellon University (1999).

[13] T. Kimoto, A. Itoh, and H. Matsunami, Phys. Stat. Solidi B **202**, 247 (1997).

[14] H. Saitoh, A. Manabe, and T. Kimoto, Mat. Sci. Forum **527-529**, 223 (2006).

[15] T. Kimoto, A. Itoh, H. Matsunami, and T. Okano, J. Appl. Phys. **81**, 3494 (1997).

[16] N. Ohtani, M. Katsuno, J. Takahashi, H. Yashiro, M. Kanaya, Phys. Rev. B **59**, 4592 (1999).

[17] E. D. Williams and N. C. Bartelt, Science, **251**, 393 (1991).

[18] J. Mysliveček, C. Schelling, F. Schäffler, G. Springholz, P. Šmilauer, J. Krug, B. Voigtländer, Surf. Sci. **520**, 193 (2002).